ELSEVIER

International Journal of Mass Spectrometry 176 (1998) 125–131

International Journal of Mass Spectrometry

# Sputter induced topography on silver coated silicon nitride ceramics by unfocused neutral primary beam selected ion mass spectrometry

W. Dümmler[a,*], S. Weber[a], N. Maloufi[b], C. Tête[a], S. Scherrer[a]

[a]*Laboratoire de Physique des Matériaux, URA 155, Ecole des Mines, Parc de Saurupt, F-54042 Nancy, France*
[b]*Université Henry Poincaré de Nancy I, B.P. 239, 54506 Vandeuvre, France*

Received 11 February 1998; accepted 16 March 1998

**Abstract**

In a specially modified apparatus for secondary ion mass spectrometry, silver-coated and uncoated silicon nitride ceramics were sputtered by means of unfocused neutral particle bombardment. The roughnesses of the obtained craters were measured by atomic force microscopy, in order to examine changes of the surface topography as a function of eroded depth. The unfocused neutral particle bombardment of a silver-coated silicon nitride ceramic was found to change the crater bottom roughness in a different way in the silver layer and the silicon nitride bulk, and the highest roughness was found to occur just at the interface. (Int J Mass Spectrom 176 (1998) 125–131) © 1998 Elsevier Science B.V.

*Keywords:* Secondary ion mass spectrometry; Surface roughness; Atomic force microscopy; Silicon nitride; Insulator

## 1. Introduction

The intense activities in recent years in the area of engineering application of ceramics have led to a growing interest in joining metals to ceramics. Today, one of the most promising ceramics is silicon nitride ($Si_3N_4$), often regarded as a class of materials comparable to steel [1]. Most of the filler metals, used for joining $Si_3N_4$ to other metals or ceramics, are based on compounds containing Ag, Ti, and Cu. The quality of the bonding depends strongly on the reactions that take place in the interfacial region. Consequently, the interfacial microstructures of the $Si_3N_4$/metal joints have been studied extensively in the past years [2].

This article is a part of a larger programme, in which diffusion of the elements Ag, Ti, and Cu into the ceramic silicon nitride has been studied by means of secondary ion mass spectrometry (SIMS). It is well known that beam-induced surface roughening during sputter depth profiling analysis deteriorates the depth resolution [3,4]. On the surface of polycrystalline materials, cone formations relative to the incident beam have been observed [5], due to different sputtering rates depending on the grain orientations [6].

The aim of this article is to show that depth profiling by sputtering of a metal–ceramic interface can provoke a changing behaviour of roughness development. As a result of previous studies on SIMS

* Corresponding author.


*PII* S1387-3806(98)14033-2

analysis of insulating materials, the neutral primary beam method (SIMS/NPB) has been developed in our laboratory [7]. The bombardment with a beam of neutral argons allowed, in particular, depth profiling of interfaces from conducting to isolating materials without deteriorations from charge effects.

For a better understanding of the results obtained in this study, we provide some main features of the silicon nitride structure. Silicon nitride ceramic is a highly covalent bonded compound that is densified by liquid phase sintering using metal oxides as additives ($Al_2O_3$ and $Y_2O_3$ for example). During sintering, the oxides react with $SiO_2$—always present at the surface of $Si_3N_4$ particles—to form an oxide melt and an oxynitride melt by dissolution of $Si_3N_4$ with increasing temperature. The resulting microstructure consists of elongated $Si_3N_4$ needles embedded in a matrix of smaller equiaxed $Si_3N_4$ grains and a grain boundary phase [8]. This grain boundary phase, often described as a glassy phase [1,9], influences the physical and chemical properties of the ceramic [10].

## 2. Experimental

The manually polished silicon nitride wafers were silver coated by vapour deposition. The deposition rate was 0.3 nm/s and the layer thickness was 350 nm, as confirmed by surface profilometer measurements of an abrupt step of coated to uncoated surface, using a Dektak measuring system (Sloan Technology Corporation).

The sample surfaces were sputtered by a non-scanned, unfocused primary beam of argon neutrals with an impact energy of 10 keV using the SIMS/NPB equipment mentioned above. It consists of a CAMECA SMI 300 system with modifications on accelerator electrode and sample holder [11,12]. The angle of primary beam incidence was 45°, and a mask restricted the sputtered area to a circular zone of 0.8 mm in diameter. The working pressure in the analysis chamber was about $3 \times 10^{-6}$ mbar.

Both for the coated and uncoated ceramic samples, craters of different depths, i.e. with different bombarding times, were elaborated on the same sample.

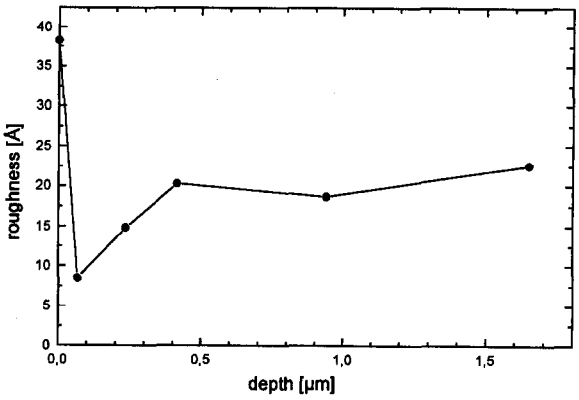


Fig. 1. Crater bottom roughness as a function of sputtered depth of a silicon nitride sample.

This ensures equal initial surface conditions for the different craters obtained.

To measure the roughnesses of the crater bottoms we used atomic force microscopy (AFM; Auto Probe CP apparatus, Park Scientific Instruments). The operating mode was in air at room temperature with contact at constant force (~0.16 N/m). A scanner of 5 $\mu$m distance was used to move the sample. The silicon tip (sharpened ultralever UL06A, typical radius of curvature ~100 Å) was regularly changed. The image processing was performed with the PSI Proscan 1.3 software (Park Scientific Instruments). It allowed us to calculate the root mean square roughness (rms) of the topography heights over the entire scanned area. This value represents the standard deviation of the data and is usually defined as

$$\text{rms} = \sqrt{\frac{\sum_{I=1}^{N}(z_i - \bar{z})^2}{N-1}}$$

where $N$ denotes the total number of image points, $z_i$ the height of the $i$th point, and $\bar{z}$ the mean height, calculated as $\bar{z} = (1/N)\ \Sigma_{i=1}^{N}\ z_i$.

## 3. Results and discussion

For an uncoated silicon nitride sample, the surface roughness of the AFM-scanned area on the crater bottom is plotted against the crater depth (Fig. 1). The roughness, initially about 38 Å, decreases strongly

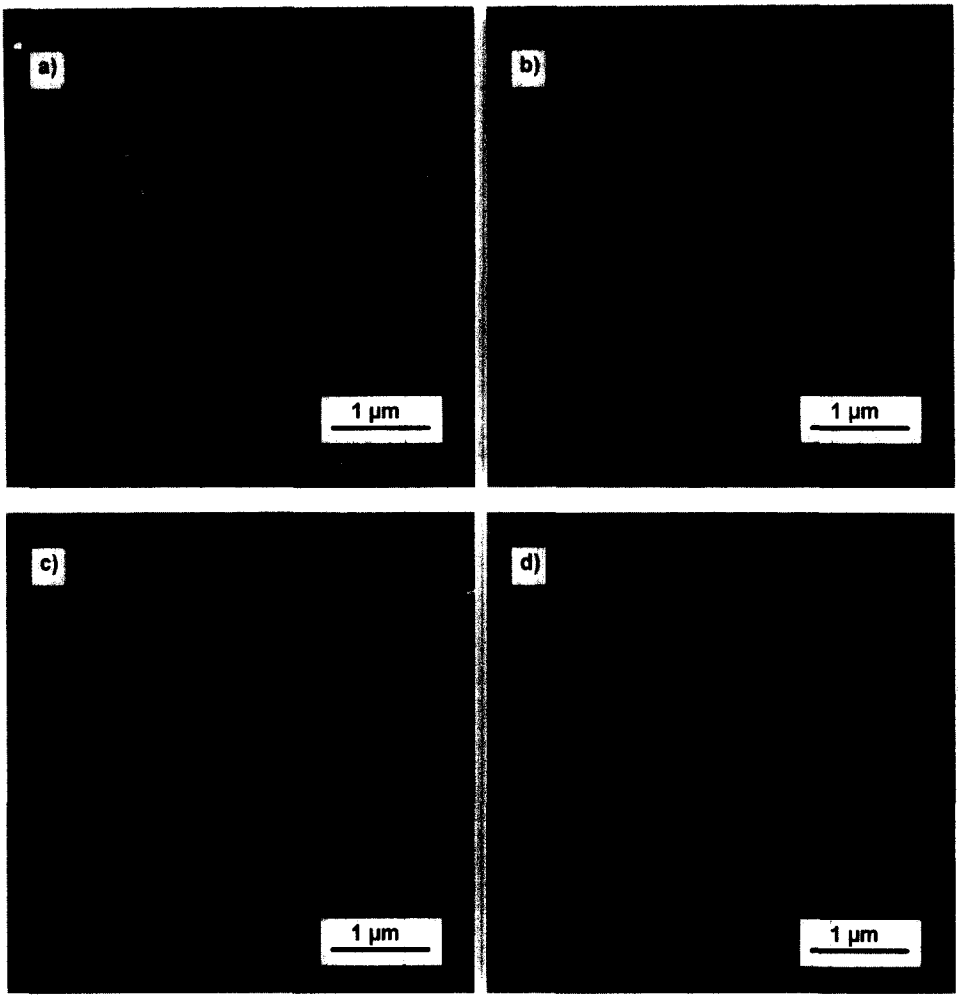


Fig. 2. AFM gray scale images of a silicon nitride surface (a) before sputtering and of bombardment-induced formation of craters with a depth of (b) 0.07 µm, (c) 0.23 µm, and (d) 0.41 µm. The scan area is 5 µm × 5 µm.

during the bombardment until reaching a depth of almost 100 nm. Then it increases within a further depth of 400 nm and remains almost constant afterward with continued bombardment. The polishing of the $Si_3N_4$ ceramic may have created an amorphous layer of silicon nitride particles, mixed with impurities at the surface. The sputtering first has to remove this layer before reaching the heterogenous $Si_3N_4$ structure with crystalline grains and amorphous grain boundary phases. Erosion of such an amorphous surface of covalent material leads to surface smoothing and thus a decreasing roughness.

In Fig. 2(a) the AFM image of a silicon nitride surface before neutral particle bombardment shows small, ball shaped grains that are significant for an amorphous structure. Fig. 2(b) represents the surface state after sputter removal of 0.07 µm. The amorphous layer has been removed after this 0.07 µm and the silicon structure of the $Si_3N_4$ appears. The ceramic structure has become even more clear at a depth of 0.23 µm [Fig. 2(c)]. The amorphous grain boundary phase, mainly consisting of silicon dioxide, mixed with metal oxides of the sintering additives, appears as deepenings between the silicon nitride grains. This means that the sputter erosion rate of these intergranular phases, mainly consisting of silicon oxide, is

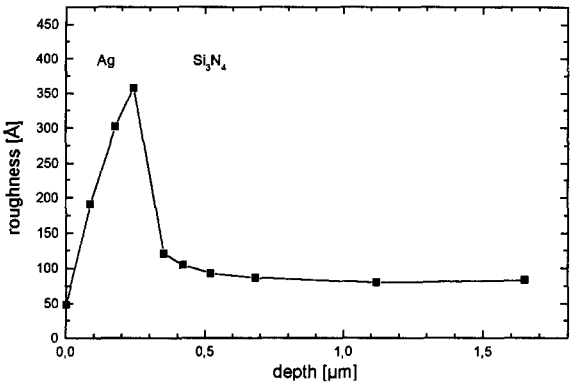


Fig. 3. Crater bottom roughness of a silver-coated silicon nitride sample as a function of sputtered depth.

obviously much higher than that of the silicon nitride grains. The comparison of the sputter erosion rates of quartz glass ($SiO_2$) $v_{SiO_2} \cong 2.3$ Å/s and of $Si_3N_4$ ceramic $v_{Si_3N_4} \cong 0.6$ Å/s, measured under equal experimental conditions with our SIMS/NPB apparatus, confirms this conclusion.

With further bombardment, the roughness increases slightly, as plotted in Fig. 1. The AFM image of a 0.94-µm depth crater bottom [Fig. 2(d)] shows the reinforced heterogenous structure of the silicon nitride, embedded in the grain boundary phase, which is represented by dark holes and ruts. This means that less amorphization of the surface during sputtering takes place, as is the case of sputtering a crystalline silicon surface [13].

In Fig. 3 the roughness dependence of the crater depth for a silver-coated silicon nitride wafer is plotted. The initial silver surface roughness represents a relatively low roughness of 48 Å. The analysis of the corresponding AFM image [Fig. 4(a)] reveals a fine grained topography of the silver surface. Sputtering with an unfocused beam of argon neutrals leads to a rising roughness of the silver surface. This is not a surface cleaning process comparable to the case of a uncoated silicon nitride surface as discussed above. It is explained by locally different sputter erosion rates, caused by defects in surface composition or different grain orientations. It has been reported [14] that varying sputtering rates can let rise bumps on a surface during bombardment. Reasons for locally different sputtering rates may also be a discontinuous film of oxides, mechanical damage, or other contaminations on the silicon surface, such as Ta sputtered from the beam defining aperture or the sample mask onto the bombarded area [15].

Hoffman [3] states that the surface roughness rms due to different grain orientations must approximately scale with the square-root of eroded depth $z$. For the sputtering of polycrystalline samples, the dependency is reported by Marton [6] to be rms $\propto (z)^a$ with $0.5 < a < 1$. During sputtering of the silver layer, our results of the roughness confirm this dependency for $a = 0.75$ and a factor of proportionality of about 0.9, if we subtract the initial surface roughness of 50 Å.

The surface roughness rises to 360 Å until reaching the interface region. The AFM images in Fig. 4(b) and 4(c) (crater depths of 0.09 µm and 0.24 µm) show, beside this rising topography, that a preferential direction of the surface grain orientation is formed during sputtering. This is due to the mentioned 45° oblique incidence of the unfocused beam.

The topography, which rose during the silver sputtering, is suppressed during and after interface transition, which is explained by the rapidly decreasing sputter erosion rate at the interface. The sputtering rate is $v_{Ag} \cong 2.1$ Å/s in the silver layer and $v_{Si_3N_4} \cong 0.6$ Å/s in the silicon nitride. Thus, after passing the interface, sites are sputtered more slowly where the silver is removed and the ceramic appears, and still silver-covered sites are sputtered with the unchanged rate. Because of this different erosion rate, the surface roughness decreases from ≅360 to ≅105 Å, until the silver is entirely removed at a total depth of 0.42 µm. Continued sputtering smoothes the surface only slightly, with the main topographic shape conserved. The roughness decrease at the interface thus reflects the difference of sputtering rate, as can be seen by comparing the ratio of the roughnesses before and after passing the interface with the respective ratio of the erosion rates:

$$\frac{\text{rms}_{\text{before interface}}}{\text{rms}_{\text{after interface}}} = \frac{360\ \text{Å}}{105\ \text{Å}} = 3.4$$

and

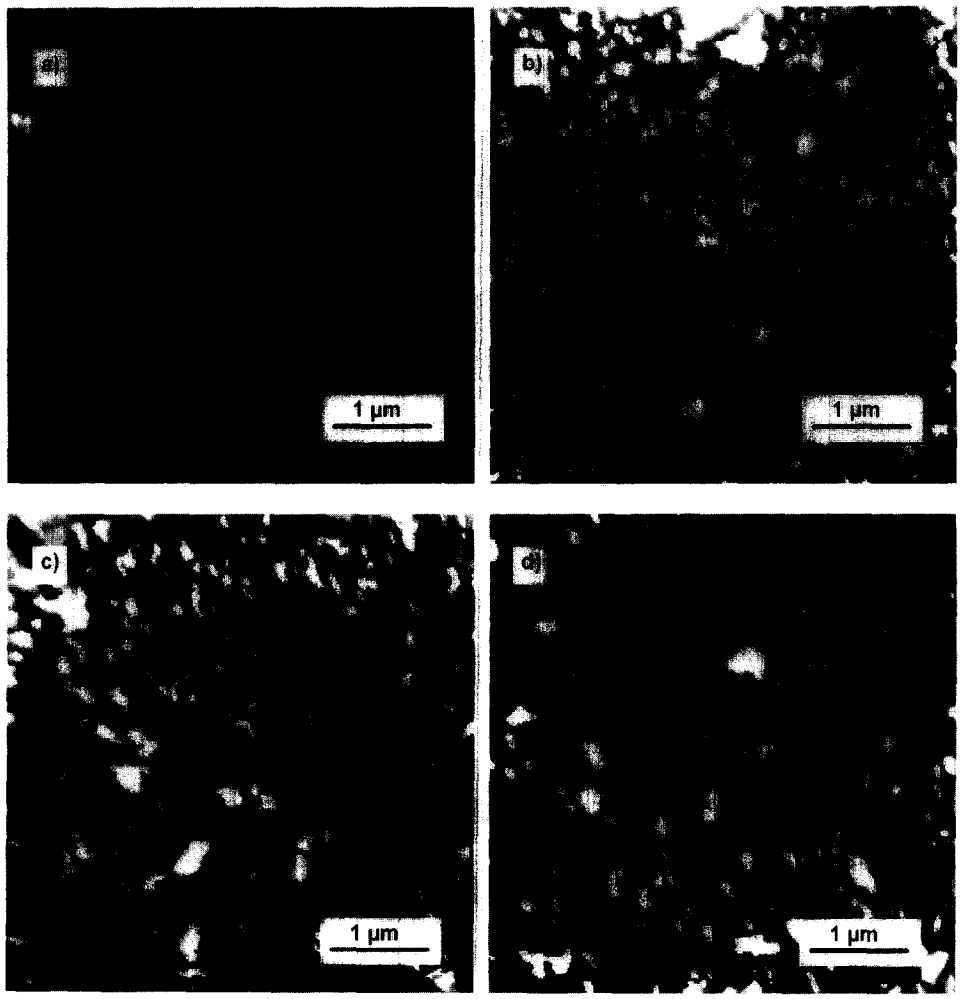


Fig. 4. AFM gray scale images of a silver-coated silicon nitride surface (a) before sputtering and of bombardment-induced formation of craters with a depth of (b) 0.09 µm, (c) 0.24 µm, and (d) 0.35 µm. The scan area is 5 µm × 5 µm.

$$\frac{v_{Ag}}{v_{Si_3N_4}} = \frac{2.1\ \text{Å/s}}{0.6\ \text{Å/s}} = 3.5.$$

The AFM images in Fig. 5(a) and 5(b) at crater depths of 0.42 µm and 1.6 µm show similar aspects as are in Fig. 2(b) and 2(d), discussed above in the context of sputtering of an uncoated $Si_3N_4$ wafer. The silicon nitride grain structure forms during sputtering of the ceramic because of the considerable difference in the erosion rate of the silicon nitride grains and the glassy grain boundary phase, as mentioned above. The silicon nitride structure appears less clear and only partly because of the conserved roughness after the interface passage. Thus, Fig. 5(b) shows some clearer regions, corresponding to a higher crater bottom level, and some darker and even black parts of former surface depressions.

## 4. Conclusions

Silver-coated and uncoated, manually polished, silicon nitride ceramics have been bombarded with an unfocused beam of argon neutrals in an apparatus for SIMS analysis. The roughnesses of crater bottoms of different depths have been measured by means of AFM.

For the uncoated silicon nitride samples, the bom-

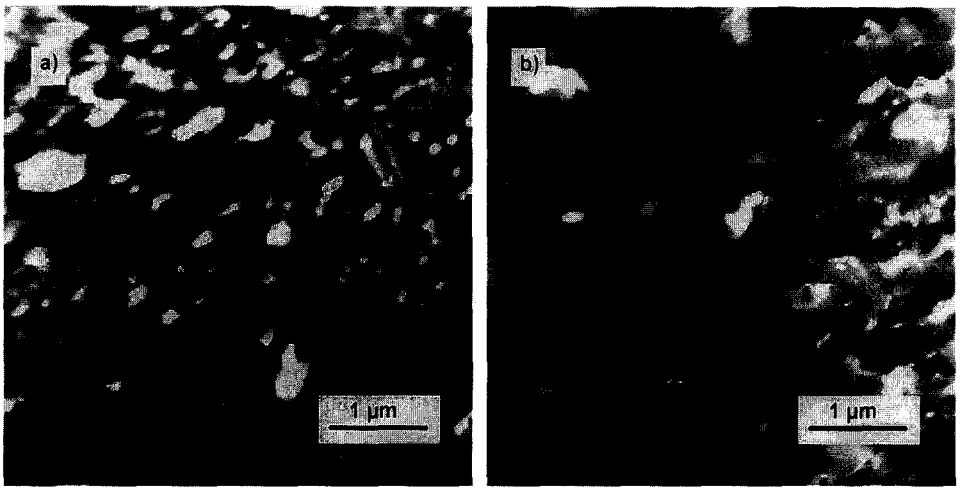


Fig. 5. AFM gray scale images of sputtered craters on a silver-coated silicon nitride surface with a depth of (a) 0.42 µm and (b) 1.60 µm. The scan area is 5 µm × 5 µm.

bardment first removes a thin, amorphous surface layer of silicon nitride grains, oxides, and impurities, formed during the sample polishing. Because of the different sputter erosion rates of $Si_3N_4$ grains and the glassy grain boundary phase, the microstructure, consisting of embedded $Si_3N_4$ grains, appears clearly. This means that the microstructure of the ceramic is not modified, contrary to the case of uncoated silicon wafers. With further bombardment, the surface roughness increases only slightly.

Bombardment of the silver-coated silicon nitride wafers first causes the surface roughness to rise. Passing the interface, the crater bottom roughness decreases sharply because of the lower sputtering rate of the ceramic. The $Si_3N_4$ microstructure is revealed only partly because of surface irregularities that were developed during the silver layer sputtering and transferred into the ceramic.

It is important to note that the highest surface roughness during sputtering of this bilayer system (metal–nonmetallic material with a heterogenous structure) is found to occur at the interface. Thus, the interim roughness during depth profiling of a layer system may be considerably higher, mainly because of different sputtering rates, than the initial and final crater bottom roughnesses. In this case the depth resolution is deteriorated and the measured profile is broadened, which must not be interpreted as reactions or diffusion phenomena of the elements in the interface region.

## Acknowledgements

The authors wish to thank R. Martin-Lopez for sample polishing. W. Dümmler acknowledges the French Government for a scholarship.

## References

[1] T. Licko, Z. Lences, Ceramics-silikáty 38 (1994) 105.
[2] M. Paulasto, J.K. Kivilahti, Scr. Metallurgica Materialia 32 (1995) 1209.
[3] S. Hofmann, Progr. Surf. Sci. 36 (1991) 35.
[4] K. Wittmaack, in D. Briggs, M.P. Seah (Eds.), Practical Surface Analysis, Vol. 2, Ion and Neutral Spectroscopy, 2nd ed., Wiley, Chichester, 1992, Ch. 3.
[5] M. Tanemura, S. Fujimoto, F. Okuyama, Surf. Interface Anal. 15 (1990) 537.
[6] D. Marton, J. Fine, Thin Solid Films 151 (1987) 433.
[7] G. Borchardt, H. Scherrer, S. Weber, S. Scherrer, Int. J. Mass. Spectrom. Ion Phys. 34 (1980) 361.
[8] M.J. Hoffmann, MRS Bull., Feb. (1995) 28.
[9] C. Greskovich, S. Prochazka, J.H. Rosomowski, in F.L. Riley (Ed.), Nitrogen Ceramics, Proc. NATO Adv. Study Inst., Série: Appl. Sci. 23, Nordhoff, Leyden, 1977, p. 351.
[10] I. Fanderlik, in A. Koller (Ed.), Structure and Properties of

Ceramics, Elsevier Science, Amsterdam, 1994, Chap. 7, p. 346.
[11] S. Scherrer, F. Naudin, Proc. XI Int. Glass Congress Prague, 4–7 September 1977, CVTS-DVM Techniky Prague, 1977, Vol. 3, p. 301.
[12] G. Borchardt, S. Scherrer, S. Weber, Microchim Acta 2 (1981) 421.
[13] W. Dümmler, N. Maloufi, S. Weber, C. Tête, S. Scherrer, Int. J. Mass Spectrom. Ion Processes 173(1988) 99.
[14] A. Benninghoven, F.G. Rüdenauer, H.W. Werner (Eds.), Secondary Ion Mass Spectrometry, Wiley, Chichester, 1987, Chap. 2.1.10.
[15] I.H. Wilson, Radiat. Eff. 18 (1973) 95.